fire

MDPI

Article

Simulation of Soil Organic Carbon Dynamics in Postfire Boreal Forests of China by Incorporating High-Resolution Remote Sensing Data and Field Measurement

Tongxin Hu, Cheng Yu, Xu Dou, Yujing Zhang, Guangxin Li and Long Sun *

Key Laboratory of Sustainable Forest Ecosystem Management-Ministry of Education, College of Forestry, Northeast Forestry University, 26 Hexing Road, Harbin 150040, China; htxhtx@nefu.edu.cn (T.H.); yucheng@nefu.edu.cn (C.Y.); dx123mtr@nefu.edu.cn (X.D.); yujingzhang@nefu.edu.cn (Y.Z.); liguangxin@nefu.edu.cn (G.L.)

* Correspondence: sunl-cf@nefu.edu.cn; Tel.: +86-139-4501-6458

Abstract: Soil organic carbon (SOC) is an important component of the ecosystem carbon pool, and fire is one of the important disturbances in forest ecosystems. With global warming, there has been a gradual increase in boreal forest fires, which has a nonnegligible impact on the SOC dynamics in forests. The CENTURY model was employed in our study to simulate the changes in SOC stocks in boreal forests of the Great Xing'an Mountains, China under different fire severity conditions. Fire severity was represented by the metric of difference normalized burn ratio (dNBR) derived from 30-m Landsat-8 imageries. Changes in forest SOC stocks following fire disturbance were predicted under four future Representative Concentration Pathway (RCP) scenarios (RCP2.6, RCP4.5, RCP6.0, and RCP8.5). We found that the CENTURY model had good results in simulating the SOC stocks in the postfire of China's boreal forests. Forest SOC dynamics responded differently to fire severities and the larger SOC loss was associated with increasing fire severity. Importantly, a feedback mechanism was found between climate change and SOC stocks, which reduces SOC stocks with increasing temperatures. High-severity forest fires tended to cause serious damage to the SOC pool and delay forest SOC recovery time; after such events, forest SOC stocks cannot be fully recovered to the prefire levels (6.74% loss). In addition, higher CO_2 emissions and warmer temperatures significantly affected the recovery of SOC stocks after fire disturbance, resulting in larger SOC losses. Overall, we projected losses of 10.14%, 12.06%, 12.41%, and 15.70% of SOC stocks after high-severity fires in four RCP scenarios, respectively. Our findings emphasize the importance of fire disturbance and climate change on future dynamics of SOC stocks in China's boreal forests, providing a scientific basis for future boreal forest management and fire management.

Keywords: fire disturbance; soil organic carbon; climate change; CENTURY model

Citation: Hu, T.; Yu, C.; Dou, X.; Zhang, Y.; Li, G.; Sun, L. Simulation of Soil Organic Carbon Dynamics in Postfire Boreal Forests of China by Incorporating High-Resolution Remote Sensing Data and Field Measurement. *Fire* **2023**, *6*, 414. https://doi.org/10.3390/fire6110414

Academic Editors: Fuquan Zhang, Ting Yun, António Bento-Gonçalves and Luis A. Ruiz

Received: 8 October 2023
Revised: 23 October 2023
Accepted: 24 October 2023
Published: 26 October 2023

1. Introduction

Soil organic carbon (SOC) is an important component of the terrestrial carbon pool and is central to the in-depth study of nutrient element cycling in terrestrial ecosystems [1]. Global organic carbon is mainly stored in forest soils, with forest SOC pools accounting for 70–73% of global soil organic carbon pools [2]. SOC is environmentally sensitive and decomposes easily, and the burning of the organic matter soil layer during the fire process decomposes a large amount of soil surface organic carbon, resulting in a direct loss of SOC [3,4]. The potential changes in the SOC pool have important implications for the global carbon cycle. The frequency and severity of boreal forest fires have increased dramatically in the context of the global climate change [5], which will increase the loss of SOC [6–9]. The releasing C to the atmosphere will further warm the climate and establish a positive feedback between fire and climate change [10], which have an important impact on the carbon cycling processes of ecosystems and the climate system.

Boreal coniferous forest ecosystems are one of the globally important carbon pools [11] because of their thicker soil organic layer and higher SOC density and stocks [12]. It has an important role in the global terrestrial carbon pool [13]. Frequent fire disturbances have had a dramatic impact on boreal forest carbon pools [14,15], especially soil carbon pools [8]. Pellegrini et al. found that fire affects carbon in soils by reducing biomass inputs [16]; Mekonnen and Searle et al. showed that more frequent and more severe fires affect changes in the dominant forest species and thus SOC [17,18]. Moreover, Wang et al. showed that boreal forest SOC produces strong feedbacks to climate change [19]. Accurately predicting trends in soil carbon stocks in boreal forests has become more important to better conserve soil carbon stocks under disturbance and climate change [20–22].

Accurate estimation of predicted SOC and its variations remains a major challenge [23]. There is a high degree of spatial heterogeneity among forests, influenced by conditions such as geologic differences and cover, resulting in complexity and spatial variability in SOC. Different forest types influence SOC stocks [24], and elevation also significantly affects SOC stocks; SOC gradually increases with increasing elevation [25]. Wang et al. found spatial differences in the degree of change in Australian SOC stocks by modelling future changes in different climate scenarios [26]. Wang and Ding et al. showed that higher tree species richness increases SOC stocks [27]. Additionally, accurately defining the severity of fire areas on a large scale constrains the assessment of the SOC pool. In recent years, the increasing sophistication of remote sensing imagery technology has improved the accuracy of fire severity assessments. Many studies have achieved good results in classifying fire severity by calculating the differential Normalized Burn Radio (dNBR) using remote sensing images such as Landsat, MODIS and Sentinel-2 [28–31], to provide support for studies such as the burned area recovery. To better understand the process of SOC change, fire severity is assessed based on remote sensing imagery, and the dynamics of SOC is studied by synchronized process modelling [32], to provide a more convenient way to study the effects of fire on forest carbon balance. Using models to quantify the impact of fire on different ecosystems is helpful in studying the dynamic changes in SOC.

The CENTURY model is a biogeochemical model that simulates ecosystem C and N dynamics. The CENTURY model can be used to simulate and predict the dynamics of productivity and SOC in terrestrial ecosystems and has been applied in different regions with good results. For example, the CENTURY model's fire function has long been used in dune and forest studies [33,34]. Some studies using the CENTURY model can accurately simulate the SOC content and its dynamics and applicability in different regions under different changing conditions [35,36]. A number of studies have fully demonstrated the feasibility of the CENTURY model in China and the accuracy of SOC prediction [37,38]. According to others, the CENTURY model is reliable for predicting the impacts of climate change on terrestrial ecosystems [39]. The results of each of the above studies demonstrate that the CENTURY model is expected to provide an effective method for predicting SOC dynamics under various conditions.

However, at present, there is still little information about using the CENTURY model to investigate the soil carbon pools of China's boreal forests. The Great Xing'an Mountains region in northern China is rich in forest resources, but forest fires occur frequently, seriously affecting the balance of the forest carbon cycle. The model was used to simulate fire disturbance conditions and different management measures to simulate the dynamics of the forest carbon cycle in northern China and to provide important recommendations for forest management after the local occurrence of fire.

In this study, we assume that fires would not occur for 300 years after the fire disturbance, because studies have shown that the average fire return period in the Great Xing'an Mountains region is about 325 years [40], and it has been shown that coniferous forests have a lifespan of about 300 years [41]. In this study, we combined high-resolution remote sensing data and field measurements to evaluate the effects of fire severity on changes in SOC stocks and spatial distributions using the CENTURY model, and explored the effects of different Representative Concentration Pathway (RCP) scenarios on postfire forest

SOC stocks. The objectives of this study were to (1) tuning the model parameters for the study area to predict the dynamic changes in SOC stocks in the study area, (2) validate the accuracy of the CENTURY model under different fire severities, and (3) investigate the effects of fire severity and climate change on SOC stocks in the boreal forests of China.

2. Materials and Methods

In order to simulate the changes in SOC under future different fire severity and climate scenarios, a process-based CENTURY model was used for simulating forest SOC (0–20 cm). High-resolution remote sensing data were used for the classification of fire severity; and field measurement combined with lab analysis was used for (1) providing local parameters of the model (2) benchmarking/validation data for the model. The model was evaluated using criteria such as R^2, root mean square error (RMSE) and absolute percentage error (MAPE), and the changes in the spatial distribution of postfire forest SOC across various future climate scenarios were presented by ArcGIS.

2.1. Study Area

The burned area formed by a major forest fire that occurred on 2 May 2017, in the forest area of the Bilahe Forestry Bureau was selected as the research object for this study. The study area is located within the Bilahe National Nature Reserve in Inner Mongolia (123°4′29″~123°29′16″ E, 49°19′40″~49°38′30″ N) (Figure 1). The weather in this area is characterized by a cold-temperate continental monsoon climate, where the average temperature throughout the year remains at −1.1 °C and the annual precipitation reaches an average of 479.4 mm, which is mainly concentrated in June-August, and a frost-free period of approximately 130 d. The soil type is brown coniferous forest soils, which often undergo swamping. The soil layer is shallow and has a high content of gravel. The topography of the terrain in the study area is relatively gentle, with elevations ranging from 377 to 886 m above sea level. The protected area belongs to the temperate coniferous forest to the temperate broad-leaved forest transition zone, with *Larix gmelinii* as the dominant species, and white birch *Betula platyphylla*, *Quercus mongolica* and other companion understorey shrubs, such as *Rhododendron dauricum*, *Rhododendron tomentosum* and *Sorbaria sorbifolia*, dominate the understorey.

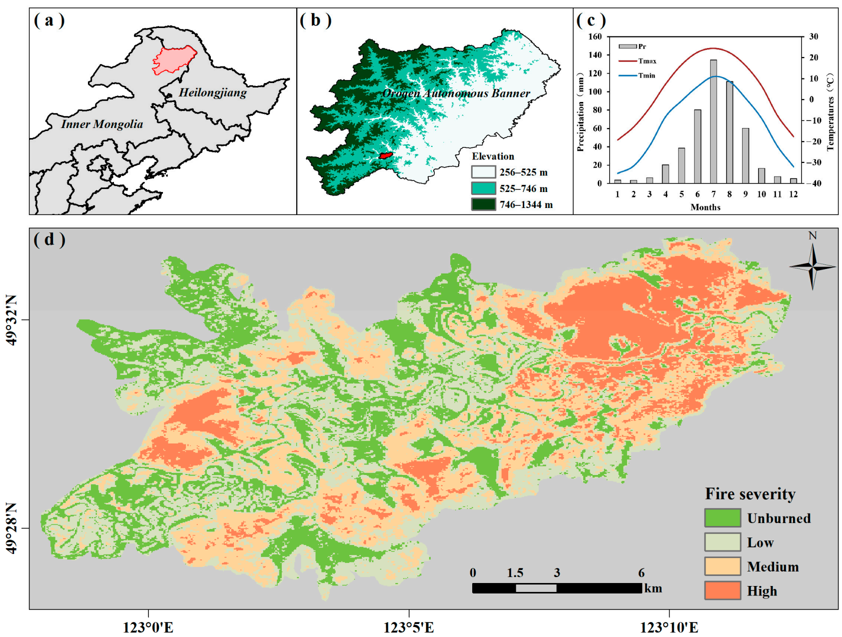

Figure 1. Location, climatic data, and fire severity classification of the study area. (**a**) Location of Oroqen Autonomous Banner; (**b**) Topographic map of Oroqen Autonomous Banner; (**c**) Climate data of the study area; (**d**) Fire severity classification.

2.2. Imagery Preprocessing and Fire Severity Classification

In this study, the Landsat8 Operational Land Imager (Landsat OLI) was used, which includes all bands of ETM+ with a spatial resolution of 30 m and a temporal period of 16 days [42]. Landsat 8 satellite images covering the study area prefire and postfire [43]. The selected images were preprocessed, radiometrically calibrated by ENVI 5.3, and atmospherically corrected using the FLAASH atmospheric correction method. The visual interpretation method was used to delineate the range of the burned area in ArcGIS and establish a vector file of the burned area and the difference normalized burn ratio (dNBR) was used to represent fire severity. The calculation formula is as follows:

$$\mathrm{dNBR} = \mathrm{NBR}_{\mathrm{prefire}} - \mathrm{NBR}_{\mathrm{postfire}} \tag{1}$$

In the formula, $\mathrm{NBR}_{\mathrm{prefire}}$ and $\mathrm{NBR}_{\mathrm{postfire}}$ denote the normalized burn ratio of the remote sensing image prefire and postfire.

The normalized burn ratio (NBR) is calculated as follows:

$$\mathrm{NBR} = \frac{(\mathrm{NIR} - \mathrm{SWIR})}{(\mathrm{NIR} + \mathrm{SWIR})} \tag{2}$$

In the formula, the NIR band denotes the near infrared band (TM5), SWIR denotes the shortwave infrared band (TM7), and the range of values for NBR is −1.0 to 1.0.

Based on the dNBR results obtained from the calculation, the fire severity of the burned area was categorized into four levels (Figure 1), including unburned ($\leq$0.1), low (0.1–0.38), medium (0.38–0.72), and high ($\geq$0.72) [29,31,44].

2.3. Soil Sampling and Analysis

A pure *Larix gmelinii* forest with similar stands was selected as the actual measurement sample plots in the fire burned areas of a *Larix gmelinii* forest, and four types of fire severity were set up: unburned, light fire severity (Low), medium fire severity (Medium) and high fire severity (High). The size of each sample plot was set at 10 m × 10 m, and six replications were set for each treatment. Within each sample plot, three points were designated for sampling, and samples were taken once in May, July and September in 2021 and 2022. The litter and humus were removed from the surface layer of each sampling site, and one cutting ring was utilized to collect soil samples from both the 0–10 cm and 10–20 cm soil layers and these samples were subsequently taken to the laboratory, where they were employed to calculate soil bulk density. Soil samples were also collected uniformly from each layer and sealed and brought back to the laboratory for the determination of soil physical and chemical properties. The soil samples to be assayed were dried naturally, and plant debris and large gravel were picked out and ground through a sieve (2 mm) for the next step of analysis. The SOC content was determined using an HT1300 total carbon analyser (Analytik Jena AG, Jena, Germany). Soil pH was determined by the potentiometric method (w (soil):w (liquid) = 1:1.25) using the pH meter (FE28-Standard). The soil texture was determined by the gravimetric method [45].

2.4. CENTURY Model Description

The CENTURY model is one of the biochemical cycling models for terrestrial ecosystems based on the interrelationships between climate, human activities, soil properties, plant productivity and decomposition of litter and soil organic matter. The model has been widely used in various ecosystems, including grassland, cropland, savanna and forest [46]. The model simulates the biogeochemical cycling of C, N, P and S based on the structural function of the soils [47]. Simultaneously, ecosystem productivity can be simulated and predicted by combining driving factors such as temperature and precipitation. For more information on the CENTURY model, visit https://www.nrel.colostate.edu/projects/century/index.php, accessed on 21 October 2021.

The main input parameters for model initialization include the average monthly maximum and minimum temperatures, monthly precipitation, soil texture, atmospheric and soil N inputs, plant lignin content and nutrient content in plants. Meteorological data were obtained from the meteorological observations of Oroqen Autonomous Banner Meteorological Stations for the years 1901–2021. The soil texture (sand content 0.22, silt content 0.35, clay content 0.43), soil bulk density, pH value and soil nutrient data were obtained from the field experiment survey (Table 1). The determination of the plant nutrient composition was based on existing studies on *Larix gmelinii* [48,49]. The atmospheric and soil N inputs use the CENTURY default parameter values. The model was applied to simulate the effect of fire on forest SOC dynamics, and in addition to set the parameters needed for model initialization, the Fire and Trem modules were also applied [34]. The FIRE module deals with the proportion of organic matter removed, the effect of fire on the increase of carbon and nitrogen ratios of aboveground and belowground tissues, and the effect of the increase of root to diameter ratios; the TREM module specifies the effect of the fire duration on the removal of plant tissues, such as the ratio of removals from trunk, branch, leaf and root.

Table 1. Soil initialization parameters in the study area (mean ± SD).

	Severity			
	Unburned	**Low**	**Medium**	**High**
SOC (t/ha)	62.01 ± 4.18	63.71 ± 3.94	64.41 ± 2.62	65.52 ± 1.62
pH	5.74 ± 0.17	5.64 ± 0.18	5.65 ± 0.22	5.83 ± 0.19
Density (g/cm^3)	1.09 ± 0.07	1.07 ± 0.08	1.11 ± 0.10	1.08 ± 0.08

2.5. CENTURY Model Calibration and Validation

Combined with existing studies, the key impact parameters were adjusted for the climatic conditions of the Great Xing'an Mountains region. Default parameters were used for most of the parameters, and adjustments were made for tree parameters (tree.100 file) and related parameters such as SOC, as well as the optimum and maximum growth temperatures, the values of which vary across regions and tree types. In this study, the parameters were tuned with reference to the mean temperature and mean maximum air temperature of the hottest month of the site. The monthly potential maximum aboveground productivity reflects the productivity of different tree species, which is one of the most important parameters for the model to be localized. After model calibration, the tree parameter values are shown in Table 2, and the Trem and Fire modules are shown in Tables 3 and 4. The calibration and validation process of the CENTURY model is shown in Figure A1.

Table 2. Calibrated values of vegetation parameters for the study area in the CENTURY model.

Parameters	Parameters Value	Description
PRDX (1)	350.000	Monthly potential maximum productivity (g/m^2)
PPDF (1)	15.000	Optimum temperature for production (°C)
PPDF (2)	36.000	Maximum temperature for production (°C)
PPDF (3)	1.000	Left arc of temperature response curve
PPDF (4)	3.500	Right arc of temperature response curve

The results of the CENTURY model simulations were thoroughly evaluated using several statistical criteria based on comparisons of observed and simulated data. Three statistical criteria were chosen for this study: correlation coefficient (R^2), root mean square error (RMSE) and absolute percentage error (MAPE) [50]. The statistical criteria are as follows:

The correlation coefficient (R^2):

$$R^2 = \left[\frac{\sum_{i=1}^{n} (Q_i - \overline{Q})(P_i - \overline{P})}{\sqrt{\sum_{i=1}^{n} (Q_i - \overline{Q})} \sqrt{\sum_{i=1}^{n} (P_i - \overline{P})}} \right]^2 \tag{3}$$

The root mean square error (RMSE):

$$\mathrm{RMSE} = \sqrt{\frac{\sum_{i=1}^{n} (P_i - Q_i)^2}{n}} \tag{4}$$

The absolute percentage error (MAPE):

$$\mathrm{MAPE} = \frac{100}{n} \sum_{i=1}^{n} \frac{|P_i - Q_i|}{\overline{Q}} \tag{5}$$

where P_i represents the simulated value and Q_i represents the observed value. $\overline{P}$ and $\overline{Q}$ are the average of the simulated and observed values, and n is the number of validation points.

Table 3. Parameters in the Trem module of the CENTURY model for different fire severities.

Fire Severity	Ratio of Aboveground Live Tissues Removed			Ratio of Underground Live Tissues Removed		Ratio of Dead Tissues Removed	
	Leaves	Fine Branch	Large Wood	Coarse Root	Fine Root	Dead Fine Branch	Dead Large Wood
Low	0.350	0.300	0.325	0.325	0.325	0.350	0.325
Medium	0.700	0.650	0.525	0.525	0.525	0.700	0.525
High	0.950	0.900	0.825	0.825	0.825	0.950	0.825

Table 4. Parameters in the CENTURY model Fire module for different fire severities.

Fire Severity	Ratio of Organics Removed			Enhanced Effect of Fire to C/N of the Above- and Underground Live Tissues		Enhanced Effect of Fire to the Root/Stem Ratio
	Standing Wood	Surface Litter	Aboveground Live Tissues	Aboveground	Fine Root	Underground
Low	0.350	0.300	0.325	0.325	0.325	0.350
Medium	0.700	0.650	0.525	0.525	0.525	0.700
High	0.950	0.900	0.825	0.825	0.825	0.950

2.6. Simulation and Data Analysis

To assess the influence of fire on SOC stocks in boreal forests for a long time, three fire severities, low fire severity (Low), medium fire severity (Medium) and high fire severity (High), were set in the Fire and Trem modules of the CENTURY model. The CENTURY model simulations predicted SOC stocks values with a temporal resolution of weeks, months, and years. The temporal resolution used in this study is months and years. The temporal changes in forest SOC stocks at different fire severities were modelled up to 300 years after fire disturbance. The future climate model chosen in this paper is the MRI-CGCM3 model in CMIP5, which has a strong ability to simulate the climate in northeast China [51], through the model's four different Representative Concentration Pathway (RCP) scenarios including RCP2.6, RCP4.5, RCP6.0, and RCP8.5. The RCPs consist of one high emission scenario (RCP8.5), two medium emission scenarios (RCP6.0 and RCP4.5) and one low emission scenario (RCP2.6). Among them, RCP8.5 leads to the largest temperature increase, followed by RCP6.0 and RCP4.5, and RCP2.6 has the smallest impact on global warming [52]. The effects of different fire severities on forest SOC stocks under different climate scenario models were explored.

Simulation results for different fire severities were compared to assess the effect of wildfires on SOC stocks in boreal forests. To assess the influence of fire severity on forest SOC stocks, the simulation results were analysed for the short term (0 to 50 years), medium term (50 to 150 years) and long term (150 to 300 years). The value of SOC stocks within each time period was calculated as the mean of all SOC values within each time period. The temporal resolution of the model over the three time periods is years. To analyse the effects of fire on the spatial distribution of SOC stocks in boreal forest, the combined effects of spatial changes in forest SOC stocks were compared for prefire, 50 years postfire, 150 years postfire and 300 years postfire.

The data analysis was processed in SPSS 22.0 (https://www.ibm.com/spss, accessed on 6 July 2022), where the data for each variable passed the normal distribution and variance homogeneity tests. The significance of the differences in SOC between the fire severity and climatic conditions and their combined effect over the three time periods were tested by analysis of variance (ANOVA). The post hoc analysis of SOC under different conditions by using the least significant difference method (LSD, $p < 0.05$) [53]. The image plotting in the article was performed in R (R4.2.3) software, and all images were analysed by the ggplot2 package [54].

3. Results

3.1. Model Validation

To validate the forest SOC stocks simulated by the CENTURY model, the simulation results were validated against the measured results. The results showed that the correlation coefficients (R^2) for Unburned, Low, Medium and High were 0.81, 0.80, 0.80 and 0.82, respectively (Figure 2). The root mean square error (RMSE) was 4.18 (t/ha), 3.94 (t/ha), 2.63 (t/ha) and 1.75 (t/ha) for Unburned, Low, Medium and High, respectively. The absolute percentage errors (MAPEs) were 5.35%, 4.84%, 3.23% and 2.25% for Unburned, Low, Medium and High, respectively.

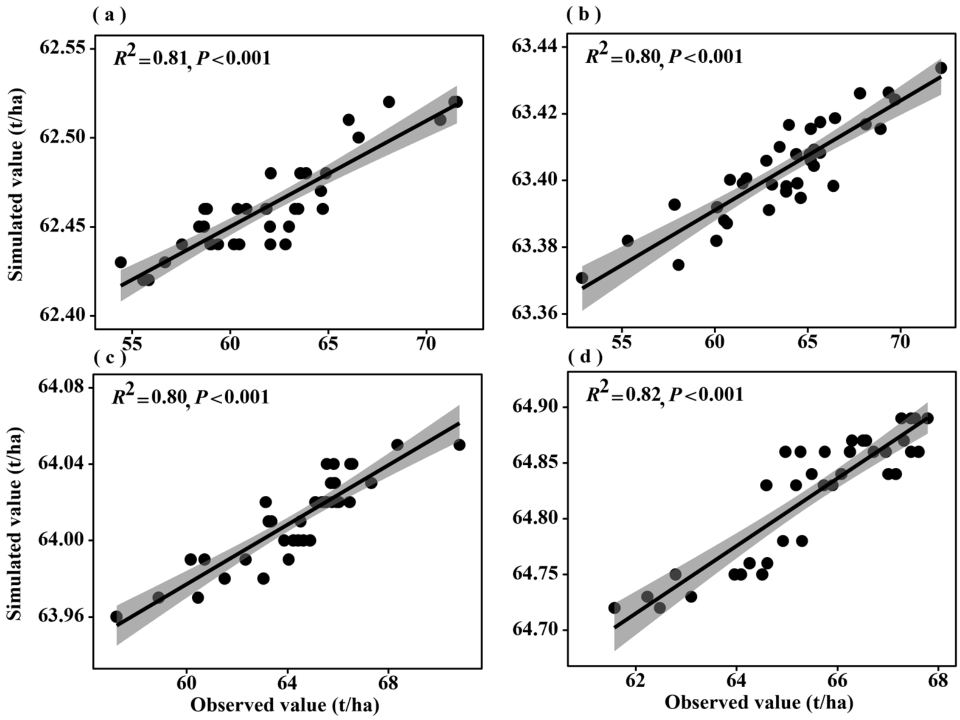

Figure 2. Comparison of SOC simulated and observed values. (**a**) unburned; (**b**) low fire severity; (**c**) medium fire severity; (**d**) high fire severity; n = 36. The lines are the fitted curves, and the gray areas represent the 95% confidence intervals.

The above results show that the R^2 between the simulated and observed values of SOC at different fire severities were high, the model deviations of RMSE and MAPE were small, and the simulation errors were within reasonable limits. It was shown that the model could better simulate the dynamic changes in SOC pools of forest in the Great Xing'an Mountains after fire disturbance.

3.2. Differential Responses of SOC to Fire Severities

Based on the ANOVA results, there was no significant difference between the simulated and observed values of SOC ($p > 0.05$), and there was a significant difference between the different fire severities (Figure 3, $p < 0.05$). The observed values of SOC stocks at different fire severities were 62.01 ± 4.18 t/ha, 63.71 ± 3.94 t/ha, 64.41 ± 2.62 t/ha and 65.52 ± 1.65 t/ha. The CENTURY model simulated SOC stocks of 62.46 ± 0.03 t/ha, 63.40 ± 0.01 t/ha, 64.01 ± 0.02 t/ha and 64.82 ± 0.06 t/ha for different fire severities.

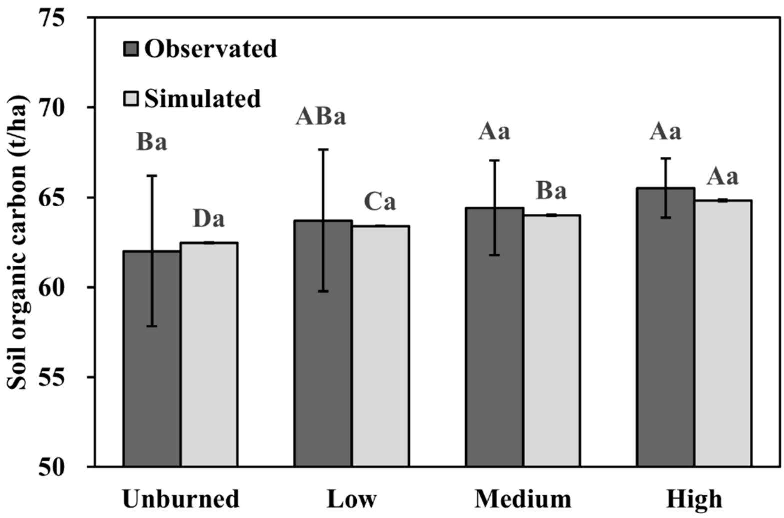

Figure 3. The results of ANOVA between simulated and observed values of SOC stocks (mean ± SD). Unburned, Low, Medium and High are different fire severities. Different lowercase letters indicate significant differences between simulated and observed values ($p < 0.05$), and different capital letters indicate significant differences in fire severity ($p < 0.05$).

3.3. Effect of Different Fire Severities on SOC

The CENTURY model categorizes soil carbon pools into active carbon pools, slow carbon pools and passive carbon pools based on different rates of carbon turnover. Analysing the changes in the SOC pools in the burned area 300 years after the fire, the three carbon pools showed different trends postfire. Within the short term after the fire, the active carbon pool rapidly increased to its peak value and then declined rapidly below the unburned level, gradually returning to the unburned level. The High had the highest SOC stocks from 0 to 18 years after the fire, and the Unburned had the highest SOC stocks from 19 to 300 years after the fire. Within the short term after the fire, the slow carbon pool also rapidly increased to its peak value and then declined rapidly below the unburned level, gradually returning to the unburned level. The SOC stocks of High were largest within 0 to 13 years after the fire, and the SOC stocks of Unburned became largest within 14 to 300 years after the fire. Within the short term after the fire, the passive carbon pool slightly increased to its peak value and then declined below the unburned level. The SOC stocks of High were highest during the first 50 years postfire and became lowest after 50 years postfire. The SOC pool (sum of active, slow and passive carbon pools) had similar trends to the active and slow carbon pools (Figure 4), and the SOC stocks in Unburned reached a maximum approximately 14 years after the fire.

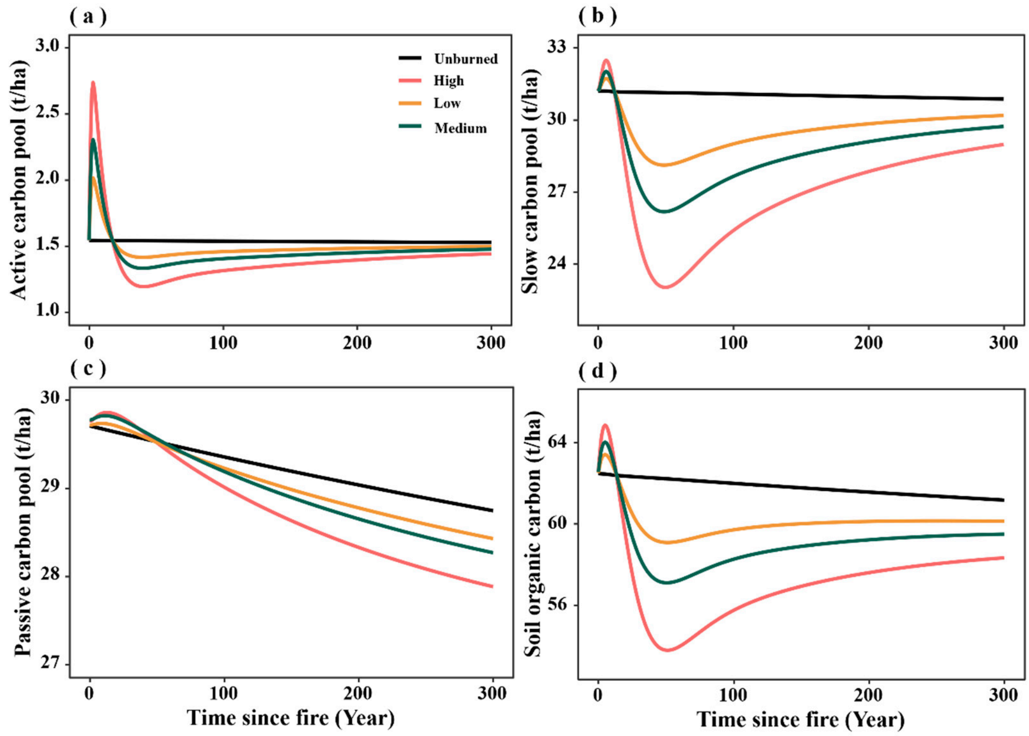

Figure 4. Changes in the relationship between SOC reserves and simulated years under different fire severities. (**a**) Activated carbon pool; (**b**) slow carbon pool; (**c**) passive carbon pool; (**d**) soil organic carbon. Unburned, Low, Medium and High are different fire severities.

There was a significant difference in SOC stocks at different fire severities ($p < 0.05$, Figure 5). In the short-term (0 to 50 years), Unburned was significantly different ($p < 0.05$) from Low, Medium and High, and there was no significant difference between Low and Medium, but both were significantly different from High ($p < 0.05$). Analysis of variance for both the medium-term (50 to 150 years) and long-term (150 to 300 years) showed significant differences ($p < 0.05$) between each fire severity.

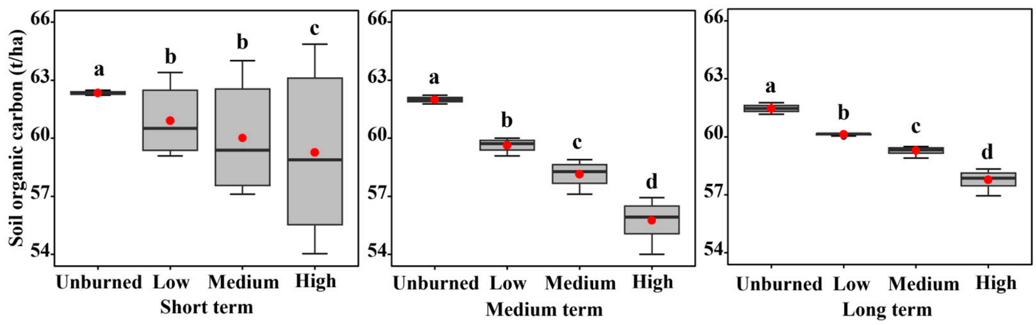

Figure 5. SOC reserves (mean ± SD) for three periods under different fire severities. Short-term: 0 to 50 years; Medium-term: 50 to 150 years; Long-term: 150 to 300 years. Unburned, Low, Medium and High are different fire severities. Different lowercase letters indicate significant ($p < 0.05$) differences between different fire severities.

Over the short, medium and long terms, there was a slight decline in the SOC stocks in Unburned, but the decrease was not significant. The SOC stocks for the three fire severities (Low, Medium and High) all exhibited short-term > long-term > medium-term variations of significant magnitude. From the above results, it could be concluded that SOC gradually recovered to unburned levels within 150–300 years after the fire, gradually approaching prefire levels.

3.4. Dynamics of Postfire SOC in Different Future Climate Scenarios

Under different climate scenarios, SOC stocks increased and then decreased over time after fire disturbance and then gradually returned to prefire levels. However, there were significant differences in SOC changes between climate scenario models, as well as significant differences in the duration of time it took for SOC to recover to stability at different fire severities (Figure 6). Under different fire severities, the SOC reduction in the RCP8.5 climate scenario mode is the highest in 300 years. The RCP4.5 and RCP6.0 scenarios are relatively similar, and there was little difference in SOC stock between them (Figure 6).

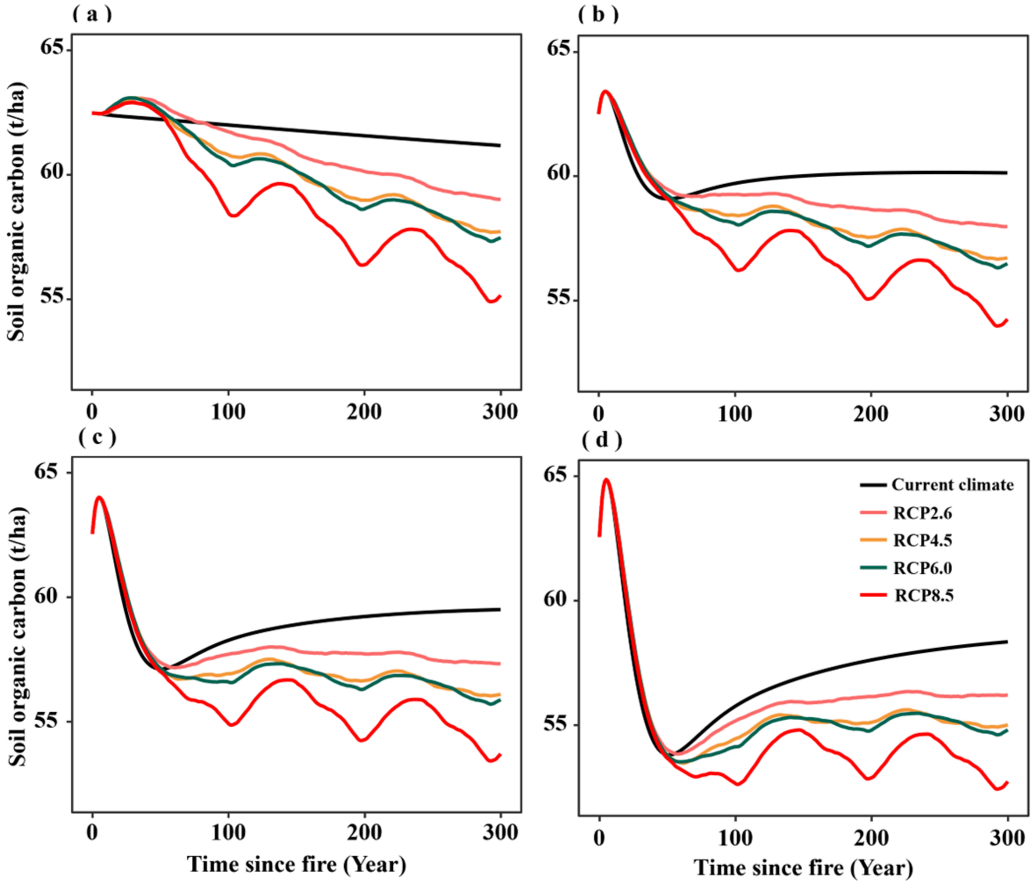

Figure 6. Changes in SOC stocks after fire under different climate scenarios. (**a**) unburned; (**b**) low fire severity; (**c**) medium fire severity; (**d**) high fire severity.

Obviously, the overall trend of SOC changes is consistent across the four climate scenarios. Over the long term, the SOC stocks of Unburned, Low and Medium still showed a decreasing trend, and the SOC of High recovered towards prefire levels (Figures 6 and 7). In the short term, the SOC had significant differences across Unburned, Low, Medium and High, but not between Low and Medium. Significant differences ($p < 0.05$) in SOC at the four fire severities were observed in the medium and long term.

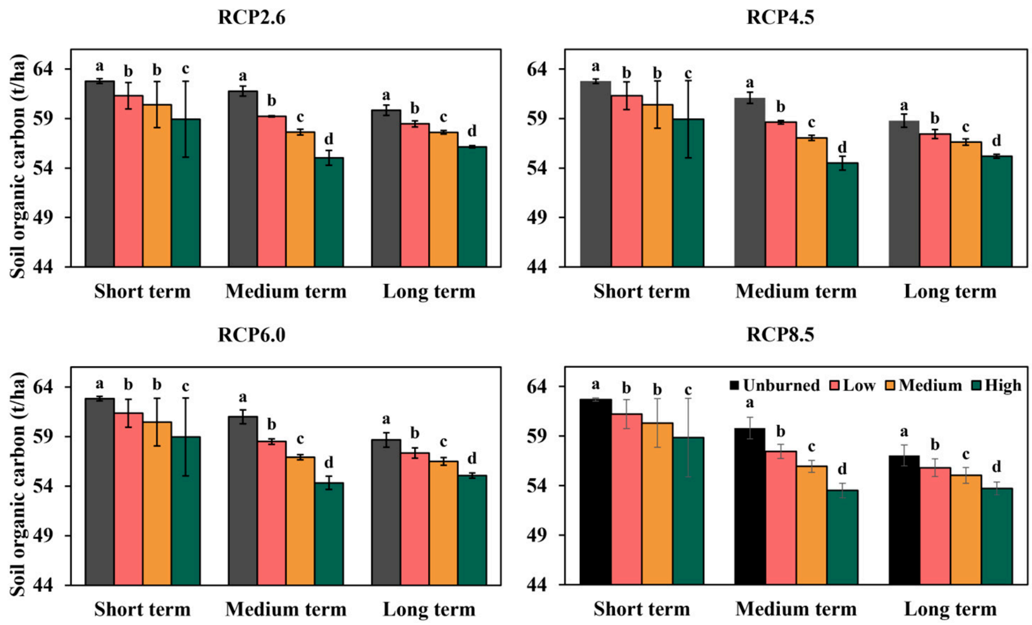

Figure 7. SOC stocks over three periods under different climate scenarios (mean ± SD). Unburned, Low, Medium and High are different fire severities. Different lowercase letters indicate significant differences between different fire severities ($p < 0.05$).

3.5. Spatial Pattern of SOC over Time

In this study area, the spatial distribution of SOC stocks in a forest were significantly different among the three periods and different climate scenario models ($p < 0.05$, Figures 8 and 9). The spatial patterns of SOC stocks at 50, 150 and 300 years postfire were significantly different at different fire severities (Figure 4). The SOC stocks under several future climate scenario models are lower than those under the current climate. The RCP4.5 and RCP6.0 scenarios are similar, so there is essentially no difference in SOC stocks between these two models. The spatial distribution of SOC stocks under several scenario models shows that temperature significantly affects SOC stocks, and carbon stocks decrease gradually with increasing temperature.

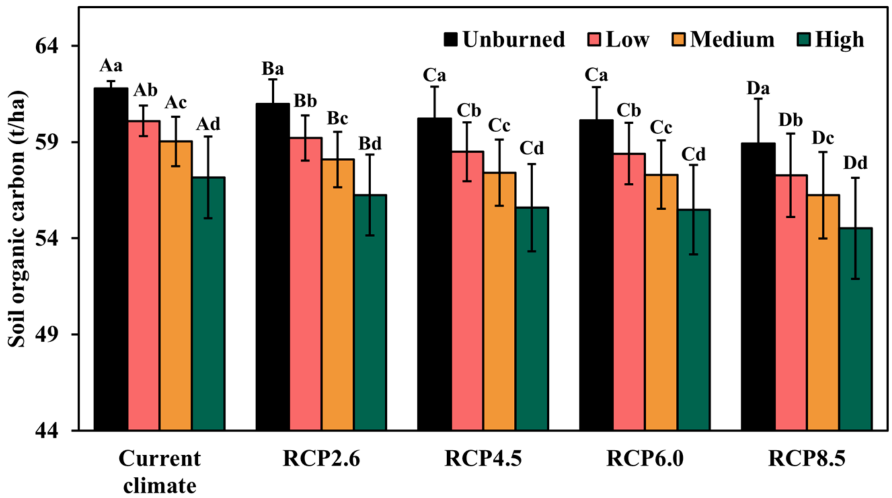

Figure 8. SOC stocks 0~300 years after fire under different climate scenarios (mean ± SD). Unburned, Low, Medium and High are different fire severities. Different lowercase letters indicate significant ($p < 0.05$) differences between different fire severities, and different uppercase letters indicate significant ($p < 0.05$) differences between different climate scenarios.

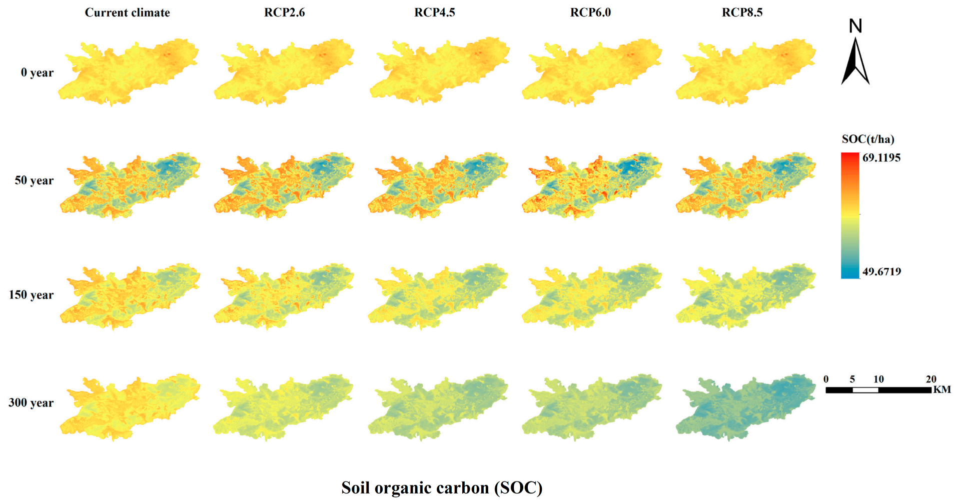

Figure 9. Spatial pattern of SOC at 0, 50, 150 and 300 years after fire under different climate scenario models.

4. Discussion

4.1. Effect of Fire Disturbance on SOC

According to our study, there was a significant effect on boreal forest SOC from fire disturbance. The observations 4–5 years after the fire showed higher SOC stocks after fire disturbance than unburned (Figure 4). This is consistent with Huang et al.'s results of predicting fire effects on SOC stocks by coupling forest ecosystem and landscape models [53]. In the short postfire period (0–14 years), SOC stocks increase with fire severity, which is likely due to the positive replenishment of the SOC pool by root death after fire disturbance [55]. Secondary succession occurs in ecosystems following fire disturbance, where the herbaceous biomass increases in the early stages of succession, herbaceous litter increases inputs to the soils and litter inputs increase the SOC pool and microbial biomass [56–58]. The study showed that the active carbon pool contributed most to SOC in temperate forest soil [59]. Because litter and microbial biomass carbon constitute the primary constituents of the soil active carbon pools [60], they cause an increase in the short-term postfire soil active carbon pool.

The gradual decrease in SOC stocks at different fire severities over the 5–51 years postfire may be due to a weakening of the replenishment effect on the SOC pool, where inputs to the soil do not fully replenish the SOC losses caused by fire. In year 15, SOC stocks at all three fire severities began to fall below unburned levels, and the amount of SOC stocks lost was positively correlated to fire severity (Figure 5). High-severity fires result in the death of trees and reduced growth rates, thus reducing the input of carbon to the soil [61]. In addition, high-severity fires alter the forest species composition and stand age [62]. As a consequence, there has been an increase in the proportion of young forest stands [63,64]. There is a significant effect on SOC stock dynamics from the stand age, especially in the surface layer (0–20 cm) [65]. The results of many studies have shown that young forests have a lower SOC content than mature forest stands [66–68]. Combining these results, the SOC stocks gradually decreased as the severity of the fire increased. During the 300-year postfire recovery process, the forest stands gradually recovered from young to mature forests, and the biomass of litter gradually increased, contributing to SOC accumulation [69,70]; therefore, SOC also increases with stand age [71]. As a result, SOC stocks are gradually recovering to prefire levels [72]. The above results indicated that vegetation is one of the important factors affecting the soil carbon cycle [73], and it is necessary to consider changes in vegetation and disturbance to enhance the precision of estimates for forest SOC stock.

From the simulation results, it is shown that the trend of SOC after disturbance with different fire severities is basically the same; all of them increased for a short term after disturbance and then decreased to the lowest point and then they gradually tended to the unburned level, but when they reached the steady state were significantly lower than in the unburned state, especially for medium and high severity fires. In the natural recovery state, the ecosystem carbon cycle can eventually return to a steady state over a sufficiently long period of time and not differ significantly from the predisturbance state [20,74,75]. The recovery time varies among different ecosystems [76], and the recovery time also varies considerably at different levels of disturbance [77]. This study showed that SOC recovery takes the longest time under high-severity fire conditions, and the study shows a positive correlation between the recovery time and disturbance severity [20]. If human intervention is involved, it may accelerate the process of ecosystem carbon cycle recovery [78]. For instance, the results of numerous studies have shown that afforestation promotes the accumulation of SOC stocks [65,79–81]. In the postfire recovery management of boreal forest SOC, the recovery process can be accelerated by human interventions such as replanting and rebuilding in the burned area. By understanding the impacts and recovery status of different levels of fire on the SOC of China's boreal forests, it is hoped that a theoretical basis can be provided for the future management of forest fires and the management of entire boreal forests.

4.2. Effect of Climate Change on SOC

Understanding the spatial and temporal changes in forest SOC and its response to climate change can help us to improve our understanding of the forest carbon cycle, thereby offering a scientific foundation for effective forest management and utilization. By modelling different scenarios of climate change, it was found that SOC stocks decrease with increasing temperature (Figure 6). In the context of climate change, climatic factors such as temperature and precipitation can have a significant impact on SOC stocks [7,82,83]. This may be because higher temperatures accelerate the decomposition of SOC, releasing carbon dioxide into the atmosphere and resulting in lower SOC stocks [10,60]. However, this was mainly due to a warmer climate, which increased soil respiration and led to a significant decrease in SOC [84]. Under the climate change scenario, SOC stocks decrease with increasing temperature [6,7,85]; these findings are in line with what has been revealed in this article. In addition, we found that increasing temperatures exacerbate the loss of SOC from fire disturbance and that climate change forms a negative feedback adjustment to SOC stocks. Climate change also affects the time it takes for the SOC to return to a steady state after a fire. However, 300 years after the fire, due to the impact of future climate scenarios, the unburned and low fire severity areas SOC stocks have not yet reached a stable state, and the changes after 300 years are still unclear. The complexity of climate change impacts on SOC requires us to take a closer step in studying how climate change affects SOC.

The results of the study suggest that fire disturbance and climate change have reduced the organic carbon stocks of soil, which implies that a considerable amount of the carbon sequestered in soil is ultimately released back into the atmosphere, which could negatively affect the regional carbon balance and further exacerbate carbon loss. In addition, fire disturbances can cause significant tree mortality, which can lead to a substantial decline in the ecosystem services provided by forests [86]. Forest management should take into account the impact of disturbances on forest carbon dynamics, as well as focus on enhancing forest ecosystem productivity, bolstering resilience against climate change and minimizing carbon loss.

4.3. Uncertainty of SOC Spatial Distribution

The impact of fire and climate change on boreal forest SOC is an issue of great ecological and economic significance. The results show that the spatial distribution of SOC changed significantly with time at different fire severities (Figure 9), and the SOC stocks under different climate scenarios are also significantly different [87]. In the present study, we utilized the dNBR as an auxiliary variable for spatial interpolation. The spatial distribution accuracy of SOC stocks was improved using the Co-Kriging method (CKM) [88,89]. From the interpolation results, the SOC stocks in the medium and high fire severity areas decreased slightly from the prefire level 300 years after a fire, but the SOC stocks in the unburned and low fire severity areas increased after 300 years, and the reason for this result may be the influence of the selected auxiliary variables. The density of auxiliary variable points can significantly affect the prediction accuracy of CKM interpolation [90]. Therefore, we will choose high-density auxiliary variables for interpolation as much as possible in the future to reduce the interpolation error.

The simulation results of this study are consistent with the field observations, but the SOC simulated by the CENTURY model (52.87–72.20 t/ha) is lower than that of the existing study in the Great Khingan Mountains (129 t/ha). This difference in SOC could be attributed to differences in environmental conditions at the soil sampling sites, such as differences in climate, vegetation, topography and disturbance, and all of these different factors influence the differences in SOC stocks [91,92]. The setup of the model also affects the simulation results, and when the model inputs sample parameters that do not fully reflect the actual conditions in the field or when there is uncertainty in the measured data as a result of changes in management and the environment, discrepancies between the simulated and measured SOC values may occur [93,94]. The study only parameterized the effects of climate change and single fires and did not take into account other anthropogenic disturbances. The impact of human activities to SOC stocks is a much more complex process [39].

4.4. Summary and Prospects

The results of our study emphasize the significant loss of forest SOC caused by fire disturbance and the fact that increasing temperatures from climate change will further increase the loss of forest SOC. The study showed that high-severity fires cause the greatest amount of SOC loss and increased recovery time. Even when reaching steady states, a certain amount of SOC is lost, resulting in carbon loss throughout the ecosystem. With global warming in the future, extreme fire events are more likely to occur, which could leave boreal forests in a state of constant disturbance and significantly affect SOC stabilization stock. This positive climate-fire feedback exacerbates the incomplete postfire recovery. For future fire management in China, the Chinese fire departments can reduce the occurrence of high-risk and high-severity fires by prescribed burning.

In this paper, the accuracy and applicability of the CENTURY model to simulate the Great Xing'an Mountains region in northern China under various conditions are demonstrated by continuous measured data to validate the model simulation results. We quantified changes in surface (0–20 cm) SOC stocks, aiming to contribute to a better understanding of the process of SOC accumulation in China's boreal forests and thus to the exploration of global boreal forest SOC changes. In the future, research on soil carbon pools in boreal forests should also attempt to assess soil carbon pools through more refined regional assessments. Adding more sample information improves the accuracy of the simulation when making predictions over large areas and thereby reduces the uncertainty in the forest SOC. Ultimately, our study will provide a basis for exploring the interactions between climate change and disturbances and soil carbon pools and provide some reference for dual-carbon (carbon emissions peak and carbon neutrality) emission reduction in China.

5. Conclusions

In this study, the CENTURY model was used to predict SOC stocks in the boreal forests of China, and burned areas with different fire severities in the same forest fire were selected as the study area to minimize the bias of the results due to spatial heterogeneity and thereby to explore the effect of fire disturbance on SOC stocks. The CENTURY model provides insight into the dynamics of SOC stocks in China's boreal forests under different severities of fire disturbance and climate change. Our results showed that the CENTURY model could better simulate the SOC stocks in China's boreal forests. Furthermore, fire disturbance significantly reduced forest SOC stocks, which decreased progressively with increasing fire severity, and climate change exacerbated SOC loss. The above results indicate that there is some negative feedback between climate warming and forest SOC. Moreover, forest SOC stocks could not be fully restored to prefire levels after forests recovered naturally following high-severity fire disturbances. Therefore, in future forest management, the loss of forest SOC stocks should be avoided by strictly managing wildfires and reducing the probability of forest fires. In addition, human activities, forest management practices, and fire rotation periods in boreal forests should be considered in future studies to further refine the study of SOC in boreal forests.

Author Contributions: Conceptualization, T.H. and L.S.; methodology, T.H., C.Y. and X.D.; software, T.H., C.Y. and Y.Z.; validation, C.Y., X.D. and T.H.; formal analysis, T.H., C.Y. and X.D.; investigation, C.Y. and G.L.; resources, T.H. and L.S.; data curation, T.H. and C.Y.; writing—original draft preparation, T.H. and C.Y.; writing—review and editing, X.D., G.L. and L.S.; visualization, C.Y. and Y.Z.; supervision, T.H. and L.S.; project administration, T.H. and L.S.; funding acquisition, T.H. and L.S. All authors have read and agreed to the published version of the manuscript.

Funding: This research was financially supported by the National Natural Science Foundation (No. 32001324), Youth Lift Project of China Association for Science and Technology (No. YESS20210370), Heilongjiang Province Outstanding Youth Joint Guidance Project (No. LH2021C012) and Fundamental Research Funds for the Central Universities (2572023CT01).

Institutional Review Board Statement: Not applicable.

Informed Consent Statement: Not applicable.

Data Availability Statement: The data that support the findings of this study are available on request from the corresponding author, (L.S.).

Conflicts of Interest: The authors declare no conflict of interest.

Appendix A

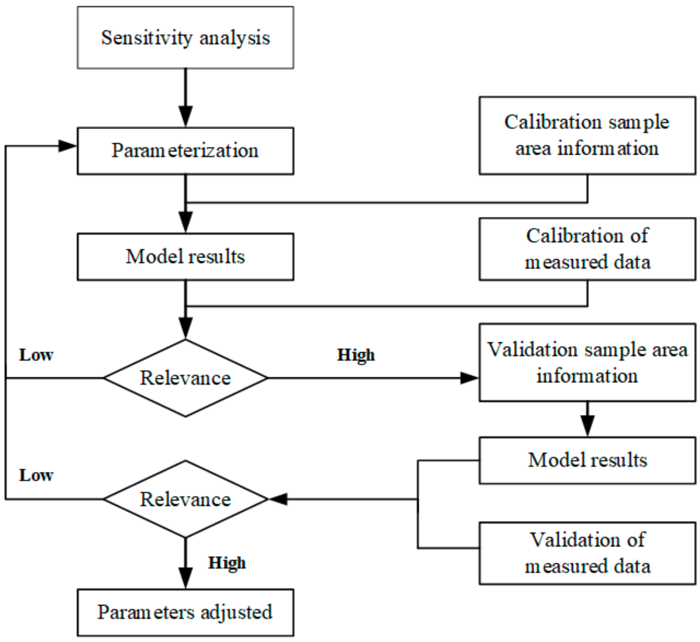

Figure A1. CENTURY model calibration and validation.

References

1. Jackson, R.B.; Lajtha, K.; Crow, S.E.; Hugelius, G.; Kramer, M.G.; Piñeiro, G. The Ecology of Soil Carbon: Pools, Vulnerabilities, and Biotic and Abiotic Controls. *Annu. Rev. Ecol. Evol. Syst.* **2017**, *48*, 419–445. [CrossRef]

2. Güner, Ş.T.; Güner, D. Changes in carbon stocks of soil and forest floor in black pine plantations in Turkey. *J. For. Res.* **2020**, *32*, 339–347. [CrossRef]
3. Certini, G.; Nocentini, C.; Knicker, H.; Arfaioli, P.; Rumpel, C. Wildfire effects on soil organic matter quantity and quality in two fire-prone Mediterranean pine forests. *Geoderma* **2011**, *167*, 191–199. [CrossRef]
4. Han, C.-L.; Sun, Z.-X.; Shao, S.; Wang, Q.-B.; Libohova, Z.; Owens, P.R. Changes of Soil Organic Carbon after Wildfire in a Boreal Forest, Northeast CHINA. *Agronomy* **2021**, *11*, 1925. [CrossRef]
5. Walker, X.J.; Baltzer, J.L.; Cumming, S.G.; Day, N.J.; Ebert, C.; Goetz, S.; Johnstone, J.F.; Potter, S.; Rogers, B.M.; Schuur, E.A.G.; et al. Increasing wildfires threaten historic carbon sink of boreal forest soils. *Nature* **2019**, *572*, 520–523. [CrossRef] [PubMed]
6. Muñoz-Rojas, M.; Doro, L.; Ledda, L.; Francaviglia, R. Application of CarboSOIL model to predict the effects of climate change on soil organic carbon stocks in agro-silvo-pastoral Mediterranean management systems. *Agric. Ecosyst. Environ.* **2015**, *202*, 8–16. [CrossRef]
7. Jebari, A.; Del Prado, A.; Pardo, G.; Rodriguez Martin, J.A.; Alvaro-Fuentes, J. Modeling Regional Effects of Climate Change on Soil Organic Carbon in Spain. *J. Environ. Qual.* **2018**, *47*, 644–653. [CrossRef] [PubMed]
8. Genet, H.; McGuire, A.D.; Barrett, K.; Breen, A.; Euskirchen, E.S.; Johnstone, J.F.; Kasischke, E.S.; Melvin, A.M.; Bennett, A.; Mack, M.C.; et al. Modeling the effects of fire severity and climate warming on active layer thickness and soil carbon storage of black spruce forests across the landscape in interior Alaska. *Environ. Res. Lett.* **2013**, *8*, 045016. [CrossRef]
9. Li, X.; Jin, H.; Wang, H.; Wu, X.; Huang, Y.; He, R.; Luo, D.; Jin, X. Distributive features of soil carbon and nutrients in permafrost regions affected by forest fires in northern Da Xing'anling (Hinggan) Mountains, NE China. *Catena* **2020**, *185*, 104304. [CrossRef]
10. Mekonnen, Z.A.; Riley, W.J.; Randerson, J.T.; Shirley, I.A.; Bouskill, N.J.; Grant, R.F. Wildfire exacerbates high-latitude soil carbon losses from climate warming. *Environ. Res. Lett.* **2022**, *17*, 094037. [CrossRef]
11. Deluca, T.H.; Boisvenue, C. Boreal forest soil carbon: Distribution, function and modelling. *Forestry* **2012**, *85*, 161–184. [CrossRef]
12. Gao, B.; Taylor, A.R.; Chen, H.Y.H.; Wang, J. Variation in total and volatile carbon concentration among the major tree species of the boreal forest. *For. Ecol. Manag.* **2016**, *375*, 191–199. [CrossRef]
13. Bradshaw, C.J.A.; Warkentin, I.G. Global estimates of boreal forest carbon stocks and flux. *Glob. Planet. Chang.* **2015**, *128*, 24–30. [CrossRef]
14. van Bellen, S.; Garneau, M.; Bergeron, Y. Impact of Climate Change on Forest Fire Severity and Consequences for Carbon Stocks in Boreal Forest Stands of Quebec, Canada: A Synthesis. *Fire Ecol.* **2010**, *6*, 16–44. [CrossRef]
15. Richardson, D.; Black, A.S.; Irving, D.; Matear, R.J.; Monselesan, D.P.; Risbey, J.S.; Squire, D.T.; Tozer, C.R. Global increase in wildfire potential from compound fire weather and drought. *npj Clim. Atmos. Sci.* **2022**, *5*, 23. [CrossRef]
16. Pellegrini, A.F.A.; Harden, J.; Georgiou, K.; Hemes, K.S.; Malhotra, A.; Nolan, C.J.; Jackson, R.B. Fire effects on the persistence of soil organic matter and long-term carbon storage. *Nat. Geosci.* **2021**, *15*, 5–13. [CrossRef]
17. Mekonnen, Z.A.; Riley, W.J.; Randerson, J.T.; Grant, R.F.; Rogers, B.M. Expansion of high-latitude deciduous forests driven by interactions between climate warming and fire. *Nat. Plants* **2019**, *5*, 952–958. [CrossRef]
18. Searle, E.B.; Chen, H.Y.H. Persistent and pervasive compositional shifts of western boreal forest plots in Canada. *Glob. Chang. Biol.* **2017**, *23*, 857–866. [CrossRef]
19. Wang, M.; Guo, X.; Zhang, S.; Xiao, L.; Mishra, U.; Yang, Y.; Zhu, B.; Wang, G.; Mao, X.; Qian, T.; et al. Global soil profiles indicate depth-dependent soil carbon losses under a warmer climate. *Nat. Commun.* **2022**, *13*, 5514. [CrossRef]
20. Fu, Z.; Li, D.; Hararuk, O.; Schwalm, C.; Luo, Y.; Yan, L.; Niu, S. Recovery time and state change of terrestrial carbon cycle after disturbance. *Environ. Res. Lett.* **2017**, *12*, 104004. [CrossRef]
21. Smith, P. An overview of the permanence of soil organic carbon stocks: Influence of direct human-induced, indirect and natural effects. *Eur. J. Soil Sci.* **2005**, *56*, 673–680. [CrossRef]
22. Batjes, N.H. Total carbon and nitrogen in the soils of the world. *Eur. J. Soil Sci.* **2014**, *65*, 10–21. [CrossRef]
23. Ťupek, B.; Launiainen, S.; Peltoniemi, M.; Sievänen, R.; Perttunen, J.; Kulmala, L.; Penttilä, T.; Lindroos, A.J.; Hashimoto, S.; Lehtonen, A. Evaluating CENTURY and Yasso soil carbon models for CO_2 emissions and organic carbon stocks of boreal forest soil with Bayesian multi-model inference. *Eur. J. Soil Sci.* **2019**, *70*, 847–858. [CrossRef]
24. Song, X.; Kimberley, M.O.; Zhou, G.; Wang, H. Soil carbon dynamics in successional and plantation forests in subtropical China. *J. Soils Sediments* **2016**, *17*, 2250–2256. [CrossRef]
25. Wu, M.; Pang, D.; Chen, L.; Li, X.; Liu, L.; Liu, B.; Li, J.; Wang, J.; Ma, L. Chemical composition of soil organic carbon and aggregate stability along an elevation gradient in Helan Mountains, northwest China. *Ecol. Indic.* **2021**, *131*, 108228. [CrossRef]
26. Wang, B.; Gray, J.M.; Waters, C.M.; Rajin Anwar, M.; Orgill, S.E.; Cowie, A.L.; Feng, P.; Li Liu, D. Modelling and mapping soil organic carbon stocks under future climate change in south-eastern Australia. *Geoderma* **2022**, *405*, 115442. [CrossRef]
27. Wang, H.; Ding, Y.; Zhang, Y.; Wang, J.; Freedman, Z.B.; Liu, P.; Cong, W.; Wang, J.; Zang, R.; Liu, S. Evenness of soil organic carbon chemical components changes with tree species richness, composition and functional diversity across forests in China. *Glob. Chang. Biol.* **2023**, *29*, 2852–2864. [CrossRef]
28. Soverel, N.O.; Perrakis, D.D.B.; Coops, N.C. Estimating burn severity from Landsat dNBR and RdNBR indices across western Canada. *Remote Sens. Environ.* **2010**, *114*, 1896–1909. [CrossRef]
29. Giddey, B.L.; Baard, J.A.; Kraaij, T. Verification of the differenced Normalised Burn Ratio (dNBR) as an index of fire severity in Afrotemperate Forest. *S. Afr. J. Bot.* **2022**, *146*, 348–353. [CrossRef]

30. Williamson, G.J.; Ellis, T.M.; Bowman, D.M.J.S. Double-Differenced dNBR: Combining MODIS and Landsat Imagery to Map Fine-Grained Fire MOSAICS in Lowland Eucalyptus Savanna in Kakadu National Park, Northern Australia. *Fire* **2022**, *5*, 160. [CrossRef]
31. Konkathi, P.; Shetty, A. Inter comparison of post-fire burn severity indices of Landsat-8 and Sentinel-2 imagery using Google Earth Engine. *Earth Sci. Inform.* **2021**, *14*, 645–653. [CrossRef]
32. Ippolito, T.; Balkovic, J.; Skalsky, R.; Folberth, C.; Krisztin, T.; Neff, J. Predicting spatiotemporal soil organic carbon responses to management using EPIC-IIASA meta-models. *J. Environ. Manag.* **2023**, *344*, 118532. [CrossRef] [PubMed]
33. Mangan, J.M.; Overpeck, J.T.; Webb, R.S.; Wessman, C.; Goetz, A.F.H. Response of Nebraska Sand Hills Natural Vegetation to Drought, Fire, Grazing, and Plant Functional Type Shifts as Simulated by the Century Model. *Clim. Chang.* **2004**, *63*, 49–90. [CrossRef]
34. Ming, F.D.; Sheng, Z.G.; Ling, J.Y.; Rui, J.B.; Zhu, X.Z.; Hua, S.X. Impact of fire on carbon dynamics of Larix gmelinii forest in Daxing'an Mountains of North-East China: A simulation with CENTURY model. *Chin. J. Appl. Ecol.* **2012**, *23*, 2411–2421. [CrossRef]
35. Chiti, T.; Papale, D.; Smith, P.; Dalmonech, D.; Matteucci, G.; Yeluripati, J.; Rodeghiero, M.; Valentini, R. Predicting changes in soil organic carbon in mediterranean and alpine forests during the Kyoto Protocol commitment periods using the CENTURY model. *Soil Use Manag.* **2010**, *26*, 475–484. [CrossRef]
36. Foereid, B.; Høgh-Jensen, H. Carbon sequestration potential of organic agriculture in northern Europe—A modelling approach. *Nutr. Cycl. Agroecosyst.* **2004**, *68*, 13–24. [CrossRef]
37. Tang, M.; Wang, S.; Zhao, M.; Qin, F.; Liu, X. Simulated Soil Organic Carbon Density Changes from 1980 to 2016 in Shandong Province Dry Farmlands Using the CENTURY Model. *Sustainability* **2020**, *12*, 5384. [CrossRef]
38. Zhang, M.; Nazieh, S.; Nkrumah, T.; Wang, X. Simulating Grassland Carbon Dynamics in Gansu for the Past Fifty (50) Years (1968–2018) Using the Century Model. *Sustainability* **2021**, *13*, 9434. [CrossRef]
39. Zhang, M.; Li, X.; Liu, X. Simulation of Grassland SOC under Future-Climate Scenarios in Gansu, China. *Land* **2023**, *12*, 1244. [CrossRef]
40. Wang, X.G.; Li, X.Z.; He, H.S. Long-term effects of different management strategies on Larix gmelinii forests in Great Hing' an Mountains after the catastrophic fire in 1987. *Chin. J. Appl. Ecol.* **2008**, *19*, 915–921. [CrossRef]
41. Liu, Z.; He, H.S.; Yang, J.; Collins, B. Emulating natural fire effects using harvesting in an eastern boreal forest landscape of northeast China. *J. Veg. Sci.* **2012**, *23*, 782–795. [CrossRef]
42. Pu, F.; Ding, C.; Chao, Z.; Yu, Y.; Xu, X. Water-Quality Classification of Inland Lakes Using Landsat8 Images by Convolutional Neural Networks. *Remote Sens.* **2019**, *11*, 1674. [CrossRef]
43. Chen, H.Y.H.; Lecina-Diaz, J.; Alvarez, A.; Retana, J. Extreme Fire Severity Patterns in Topographic, Convective and Wind-Driven Historical Wildfires of Mediterranean Pine Forests. *PLoS ONE* **2014**, *9*, e85127. [CrossRef]
44. Shuchao, L.; Xiaozhong, C.; Xianlin, Q.; Guifen, S.; Xiaotong, L.I. Remote Sensing Assessment of Forest Fire Damage Degree in Bilahe Forest Farm, Inner Mongolia. *For. Resour. Manag.* **2018**, *1*, 90. [CrossRef]
45. Papuga, K.; Kaszubkiewicz, J.; Wilczewski, W.; Staś, M.; Belowski, J.; Kawałko, D. Soil grain size analysis by the dynamometer method–a comparison to the pipette and hydrometer method. *Soil Sci. Annu.* **2018**, *69*, 17–27. [CrossRef]
46. Parton, W.J.; Schimel, D.S.; Cole, C.V.; Ojima, D.S. Analysis of Factors Controlling Soil Organic Matter Levels in Great Plains Grasslands 1. *Soil Sci. Soc. Am. J.* **1987**, *51*, 1173–1179. [CrossRef]
47. Parton, W.J.; Stewart, J.W.B.; Cole, C.V. Dynamics of C, N, P and S in Grassland Soils: A Model. *Biogeochemistry* **1988**, *5*, 109–131. [CrossRef]
48. Meng, S.; Jia, Q.; Zhou, G.; Zhou, H.; Liu, Q.; Yu, J. Fine Root Biomass and Its Relationship with Aboveground Traits of Larix gmelinii Trees in Northeastern China. *Forests* **2018**, *9*, 35. [CrossRef]
49. Widagdo, F.R.A.; Xie, L.; Dong, L.; Li, F. Origin-based biomass allometric equations, biomass partitioning, and carbon concentration variations of planted and natural Larix gmelinii in northeast China. *Glob. Ecol. Conserv.* **2020**, *23*, e01111. [CrossRef]
50. Bellocchi, G.; Rivington, M.; Donatelli, M.; Matthews, K. Validation of biophysical models: Issues and methodologies. A review. *Agron. Sustain. Dev.* **2010**, *30*, 109–130. [CrossRef]
51. Chunwei, T.; Chao, J.; Jianxin, S.; University, B.F. Evaluation of CMIP5 Models Performance on Climate Simulation in Northeast China. *Clim. Environ. Res.* **2016**, *21*, 357–366. [CrossRef]
52. Hurtt, G.C.; Chini, L.P.; Frolking, S.; Betts, R.A.; Feddema, J.; Fischer, G.; Fisk, J.P.; Hibbard, K.; Houghton, R.A.; Janetos, A.; et al. Harmonization of land-use scenarios for the period 1500–2100: 600 years of global gridded annual land-use transitions, wood harvest, and resulting secondary lands. *Clim. Chang.* **2011**, *109*, 117–161. [CrossRef]
53. Huang, C.; He, H.S.; Hawbaker, T.J.; Liang, Y.; Gong, P.; Wu, Z.; Zhu, Z. A coupled modeling framework for predicting ecosystem carbon dynamics in boreal forests. *Environ. Model. Softw.* **2017**, *93*, 332–343. [CrossRef]
54. Ginestet, C. ggplot2: Elegant Graphics for Data Analysis. *J. R. Stat. Soc. Ser. A Stat. Soc.* **2011**, *174*, 245. [CrossRef]
55. Bowden, R.D.; Deem, L.; Plante, A.F.; Peltre, C.; Nadelhoffer, K.; Lajtha, K. Litter Input Controls on Soil Carbon in a Temperate Deciduous Forest. *Soil Sci. Soc. Am. J.* **2014**, *78*, S66–S75. [CrossRef]
56. Liu, Y.; Wang, K.; Dong, L.; Li, J.; Wang, X.; Shangguan, Z.; Qu, B.; Deng, L. Dynamics of litter decomposition rate and soil organic carbon sequestration following vegetation succession on the Loess Plateau, China. *Catena* **2023**, *229*, 107225. [CrossRef]

57. Zhou, Y.; Bomfim, B.; Bond, W.J.; Boutton, T.W.; Case, M.F.; Coetsee, C.; Davies, A.B.; February, E.C.; Gray, E.F.; Silva, L.C.R.; et al. Soil carbon in tropical savannas mostly derived from grasses. *Nat. Geosci.* **2023**, *16*, 710–716. [CrossRef]
58. Feng, J.; He, K.; Zhang, Q.; Han, M.; Zhu, B. Changes in plant inputs alter soil carbon and microbial communities in forest ecosystems. *Glob. Chang. Biol.* **2022**, *28*, 3426–3440. [CrossRef]
59. Ahirwal, J.; Gogoi, A.; Sahoo, U.K. Stability of soil organic carbon pools affected by land use and land cover changes in forests of eastern Himalayan region, India. *Catena* **2022**, *215*, 106308. [CrossRef]
60. Wan, Y.; Lin, E.; Xiong, W.; Li, Y.E.; Guo, L. Modeling the impact of climate change on soil organic carbon stock in upland soils in the 21st century in China. *Agric. Ecosyst. Environ.* **2011**, *141*, 23–31. [CrossRef]
61. Murphy, B.P.; Russell-Smith, J.; Prior, L.D. Frequent fires reduce tree growth in northern Australian savannas: Implications for tree demography and carbon sequestration. *Glob. Chang. Biol.* **2010**, *16*, 331–343. [CrossRef]
62. Shanin, V.; Komarov, A.; Mäkipää, R. Tree species composition affects productivity and carbon dynamics of different site types in boreal forests. *Eur. J. For. Res.* **2013**, *133*, 273–286. [CrossRef]
63. Schoennagel, T.; Turner, M.G.; Kashian, D.M.; Fall, A. Influence of fire regimes on lodgepole pine stand age and density across the Yellowstone National Park (USA) landscape. *Landsc. Ecol.* **2006**, *21*, 1281–1296. [CrossRef]
64. GonzÁLez, M.E.; Veblen, T.T.; Sibold, J.S. Influence of fire severity on stand development of Araucaria araucana-Nothofagus pumilio stands in the Andean cordillera of south-central Chile. *Austral Ecol.* **2010**, *35*, 597–615. [CrossRef]
65. Hou, G.; Delang, C.O.; Lu, X.; Gao, L. Soil organic carbon storage varies with stand ages and soil depths following afforestation. *Ann. For. Res.* **2019**, *62*, 3–20. [CrossRef]
66. Pregitzer, K.S.; Euskirchen, E.S. Carbon cycling and storage in world forests: Biome patterns related to forest age. *Glob. Chang. Biol.* **2004**, *10*, 2052–2077. [CrossRef]
67. Liu, T.; Peng, D.; Tan, Z.; Guo, J.; Zhang, Y. Effects of stand density on soil respiration and labile organic carbon in different aged Larix principis-rupprechtii plantations. *Ecol. Process.* **2021**, *10*, 1–15. [CrossRef]
68. Deng, W.; Wang, X.; Hu, H.; Zhu, M.; Chen, J.; Zhang, S.; Cheng, C.; Zhu, Z.; Wu, C.; Zhu, L. Variation Characteristics of Soil Organic Carbon Storage and Fractions with Stand Age in North Subtropical Quercus acutissima Carruth. Forest in China. *Forests* **2022**, *13*, 1649. [CrossRef]
69. Huang, Z.; Clinton, P.W.; Davis, M.R.; Yang, Y. Impacts of plantation forest management on soil organic matter quality. *J. Soils Sediments* **2011**, *11*, 1309–1316. [CrossRef]
70. Li, Y.; Wang, Z.; Shi, W.; Yang, H. Litter quality modifies soil organic carbon mineralization in an ecological restoration area. *Land Degrad. Dev.* **2023**, *34*, 1806–1819. [CrossRef]
71. Wang, H.; Wang, J.; Zhang, Y.; He, G.; Wen, S. Spatial distribution of soil organic carbon and its response to forest growth and soil layer in Cunninghamia lanceolata plantations in mid-subtropical China. *For. Ecol. Manag.* **2023**, *545*, 121302. [CrossRef]
72. Chen, F.-S.; Zeng, D.-H.; Fahey, T.J.; Liao, P.-F. Organic carbon in soil physical fractions under different-aged plantations of Mongolian pine in semi-arid region of Northeast China. *Appl. Soil Ecol.* **2010**, *44*, 42–48. [CrossRef]
73. Laganière, J.; Boča, A.; Van Miegroet, H.; Paré, D. A Tree Species Effect on Soil That Is Consistent Across the Species' Range: The Case of Aspen and Soil Carbon in North America. *Forests* **2017**, *8*, 113. [CrossRef]
74. Yang, Y.; Luo, Y.; Finzi, A.C. Carbon and nitrogen dynamics during forest stand development: A global synthesis. *New Phytol.* **2011**, *190*, 977–989. [CrossRef] [PubMed]
75. Marrs, R.H.; Marsland, E.L.; Lingard, R.; Appleby, P.G.; Piliposyan, G.T.; Rose, R.J.; O'Reilly, J.; Milligan, G.; Allen, K.A.; Alday, J.G.; et al. Experimental evidence for sustained carbon sequestration in fire-managed, peat moorlands. *Nat. Geosci.* **2018**, *12*, 108–112. [CrossRef]
76. Jones, H.P.; Schmitz, O.J. Rapid recovery of damaged ecosystems. *PLoS ONE* **2009**, *4*, e5653. [CrossRef] [PubMed]
77. Luo, Y.; Keenan, T.F.; Smith, M. Predictability of the terrestrial carbon cycle. *Glob. Chang. Biol.* **2014**, *21*, 1737–1751. [CrossRef]
78. Magnani, F.; Mencuccini, M.; Borghetti, M.; Berbigier, P.; Berninger, F.; Delzon, S.; Grelle, A.; Hari, P.; Jarvis, P.G.; Kolari, P.; et al. The human footprint in the carbon cycle of temperate and boreal forests. *Nature* **2007**, *447*, 849–851. [CrossRef]
79. Assefa, D.; Rewald, B.; Sandén, H.; Rosinger, C.; Abiyu, A.; Yitaferu, B.; Godbold, D.L. Deforestation and land use strongly effect soil organic carbon and nitrogen stock in Northwest Ethiopia. *Catena* **2017**, *153*, 89–99. [CrossRef]
80. Li, D.; Niu, S.; Luo, Y. Global patterns of the dynamics of soil carbon and nitrogen stocks following afforestation: A meta-analysis. *New Phytol.* **2012**, *195*, 172–181. [CrossRef]
81. Song, X.; Peng, C.; Zhou, G.; Jiang, H.; Wang, W. Chinese Grain for Green Program led to highly increased soil organic carbon levels: A meta-analysis. *Sci. Rep.* **2014**, *4*, 4460. [CrossRef] [PubMed]
82. Soleimani, A.; Hosseini, S.M.; Massah Bavani, A.R.; Jafari, M.; Francaviglia, R. Simulating soil organic carbon stock as affected by land cover change and climate change, Hyrcanian forests (northern Iran). *Sci. Total Environ.* **2017**, *599–600*, 1646–1657. [CrossRef] [PubMed]
83. Mondini, C.; Coleman, K.; Whitmore, A.P. Spatially explicit modelling of changes in soil organic C in agricultural soils in Italy, 2001–2100: Potential for compost amendment. *Agric. Ecosyst. Environ.* **2012**, *153*, 24–32. [CrossRef]
84. Volk, M.; Suter, M.; Wahl, A.-L.; Bassin, S. Massive warming-induced carbon loss from subalpine grassland soils in an altitudinal transplantation experiment. *Biogeosciences* **2022**, *19*, 2921–2937. [CrossRef]

85. Xu, X.; Liu, W.; Kiely, G. Modeling the change in soil organic carbon of grassland in response to climate change: Effects of measured versus modelled carbon pools for initializing the Rothamsted Carbon model. *Agric. Ecosyst. Environ.* **2011**, *140*, 372–381. [CrossRef]
86. Wu, C.; Coffield, S.R.; Goulden, M.L.; Randerson, J.T.; Trugman, A.T.; Anderegg, W.R.L. Uncertainty in US forest carbon storage potential due to climate risks. *Nat. Geosci.* **2023**, *16*, 422–429. [CrossRef]
87. Zhang, W.; Zhang, F.; Qi, J.; Hou, F. Modeling impacts of climate change and grazing effects on plant biomass and soil organic carbon in the Qinghai–Tibetan grasslands. *Biogeosciences* **2017**, *14*, 5455–5470. [CrossRef]
88. Kim, H.-R.; Kim, K.-H.; Yu, S.; Moniruzzaman, M.; Hwang, S.-I.; Lee, G.-T.; Yun, S.-T. Better assessment of the distribution of As and Pb in soils in a former smelting area, using ordinary co-kriging and sequential Gaussian co-simulation of portable X-ray fluorescence (PXRF) and ICP-AES data. *Geoderma* **2019**, *341*, 26–38. [CrossRef]
89. Ceddia, M.B.; Villela, A.L.O.; Pinheiro, É.F.M.; Wendroth, O. Spatial variability of soil carbon stock in the Urucu river basin, Central Amazon-Brazil. *Sci. Total Environ.* **2015**, *526*, 58–69. [CrossRef]
90. Tziachris, P.; Metaxa, E.; Papadopoulos, F.; Papadopoulou, M. Spatial Modelling and Prediction Assessment of Soil Iron Using Kriging Interpolation with pH as Auxiliary Information. *ISPRS Int. J. Geo-Inf.* **2017**, *6*, 283. [CrossRef]
91. Johnson, K.D.; Harden, J.; McGuire, A.D.; Bliss, N.B.; Bockheim, J.G.; Clark, M.; Nettleton-Hollingsworth, T.; Jorgenson, M.T.; Kane, E.S.; Mack, M.; et al. Soil carbon distribution in Alaska in relation to soil-forming factors. *Geoderma* **2011**, *167–168*, 71–84. [CrossRef]
92. Dieleman, W.I.J.; Venter, M.; Ramachandra, A.; Krockenberger, A.K.; Bird, M.I. Soil carbon stocks vary predictably with altitude in tropical forests: Implications for soil carbon storage. *Geoderma* **2013**, *204–205*, 59–67. [CrossRef]
93. Smith, J.U.; Smith, P.; Monaghan, R.; MacDonald, A.J. When is a measured soil organic matter fraction equivalent to a model pool? *Eur. J. Soil Sci.* **2002**, *53*, 405–416. [CrossRef]
94. Sohi, S.P.; Mahieu, N.; Arah, J.R.M.; Powlson, D.S.; Madari, B.; Gaunt, J.L. A Procedure for Isolating Soil Organic Matter Fractions Suitable for Modeling. *Soil Sci. Soc. Am. J.* **2001**, *65*, 1121–1128. [CrossRef]